Face Boundary Extraction

Yi Xiao[1] and Hong Yan[1,2]

[1]School of Electrical & Information Engineering, University of Sydney, NSW 2006, Australia

[2]Department of Computer Engineering and Information Technology, City University of Hong Kong, Kowlon, Hong Kong
Email: yix@ee.usyd.edu.au
Fax: 61-2-93513847

Abstract In this paper, we propose a symmetry-based method for face boundary extraction from a binarized facial image, which contains a number of blobs after thresholding. The salient facial features such as eyes, mouth, and face borders are among the blobs. In our method, the symmetric axis transform is conducted on the exterior contours of the blobs in a binarized facial image by a Constrained Delaunay triangulation. A face shape is decomposed into a few components represented by the chain of three types of Delaunay triangles. The facial features are identified by the symmetry related distance analysis and then the face boundaries are traced with a group of connected Delaunay edges. With this method, face boundary with arbitrary shape can be traced precisely and small broken edges can be linked without obviously distortion.

Key words: Facial features, face boundary, symmetric axis transform, skeleton, Delaunay triangulation

1 Introduction

Extracting facial feature positions in a face has many applications from 2D and 3D human face modeling, feature-based face image compression, head pose estimation, and precise personal identifications to orthodontic applications [1,2]. It is noticed that, among these applications, only a few facial features such as eyes and mouth are frequently addressed for fine extraction [3] Among the studies above, the face boundary is one of the most important but difficult facial features to be extracted. Davies [4] ranks the chin as important as the mouth in a psychological assessment on the cue saliency of facial features. Consequently, the chin was used for geometrical proportion measurements in early human face recognition schemes [5]

Snake is widely used as face boundary tracking method, which is the active contour model proposed by Kass et al [6]. It uses a controlled continuity spline function, transforming the shape of the curve to make the energy function minimize from the initial state of the curve. The main difficulties with active contours tracing are that a

good initial estimation must be available, and that the active contour will always converge onto a solution, whether it is the desired solution or a false matching. Moreover, the calculation cost is expensive and therefore it is quite slow. To speed up the processing, Sobottka and Pitas [7] and Lam and Yan [8] used active contour snake models with curves such as an ellipse or partial ellipses to detect the face boundary.

Template matching is also a popular method to extract a face boundary. Lanitis et al [2] proposed flexible model with both shape and gray-level appearance. It is created by performing a statistical analysis over a training set of face images. A robust multiresolution search algorithm was used to fit the model to faces in new images. Akimoto et al [9] use template model to identify profile features such as chin tip, mouth, nose tip and nose bridge. The face outline is presented by spline curve passing through the bottom of the chin, the right and left cheek outlines and the pixels that have higher edge strength than a predefined threshold. The drawback of template matching for face boundary extraction is that it does not take into account the variable appearance of the objects. The extracted face boundary may deviate the real boundary.

To overcome the difficulty for integrating low-level (edge) information into a contour of an object, Hu et al [10] combined traditional edge detection and thresholding techniques with head/face models to locate the face boundaries. In their study, they made use of the a priori knowledge of the general shape of a head to organize the head and face edges into meaningful boundaries. The face boundaries consist of four parts: left, right, top and bottom face boundaries. The former three are traced according to the average intensity, edge pixels, boundary smoothing, segment labeling and repairing. Bottom face boundary is approximated by a segment of ellipse. The difficulty for this method is to determine the two ending points of the segment.

In this paper we aim at extracting an arbitrary shaped face boundary that may be broken. A symmetry-axis-based approach is proposed to track face boundaries from a grayscale face image. Based on the concept of *symmetric axis transform* (SAT), introduced by Blum [11, 12], a shape can be decomposed into a number of symmetrical parts (components) that can be quantitatively described. As the symmetric axis is both topologically equivalent to the original shape and invariant to rigid transformations [13, 14], the symmetry description of a shape has the highlights of tolerance of shape deformation [15] and small mergence of a shape [16]. The method will be suitable for arbitrary face shape analysis and overcome the breaks of face border caused by the partial merging of a face with other background areas.

2 Method

The proposed method has mainly two parts. First, symmetrical axis transform is constructed on the exterior contours of the blobs in a binarized grayscale facial image via a Constrained Delaunay triangulation, which decomposes a face shape into a few *components*. A component is quantitatively described by a chain of three types of Delaunay triangles. In order to get the desired topological structure for face boundary identification, components that are less significent to face shape are pruned by

triangle-based calculation and the inner facial features such as eyes, eyebrows, mouth and nose are identified from the symmetrical description. Second, the face boundaries are identified and extracted by the components linked to both facial feature boundaries and face boundaries.

2.1 Symmetrical axis transform of a face

2.1.1 SAT and the component

In Blumís description [12], the *symmetric axis transform* (SAT) of a shape is defined as the locus of the centers and the radii of all *maximal disks* contained in the shape. The locus of the centers constitutes the *symmetric axis* (SA). A SA point having one touching point is an *end point*. *Normal points* are SA points having two touching points, and *junction points* are points with three or more touching points The symmetric axis is divided into simplified segments. A *simplified segment* is a set of contiguous normal points bounded by either a junction point or an end point.

The segments makes a complex shape to be divided into simpler parts that can be topologically and quantitatively described. A shape will be basically subdivided into two-sided curves by using simplified segments . In this paper, we define a simplified segment together with its two-sided curves as a *component* of a shape (Figure 1). As the two curves forming a component may be different, we denote them as c_1 and c_2 respectively.

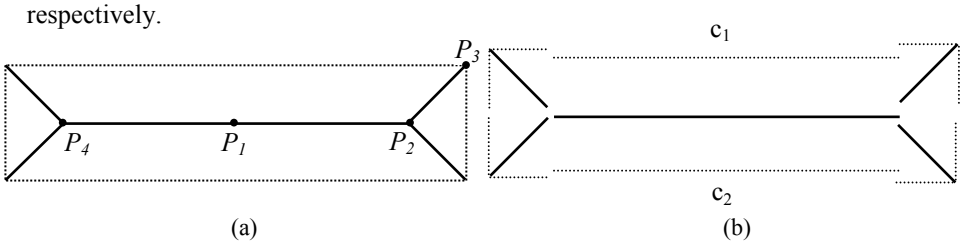

Figure 1 (a) In the symmetric axis of the rectangle, P_1 and P_3 are the normal point and end point respectively; P_2 and P_4 are junction points. (b) The symmetric axis is partitioned into five simplified segments (the solid lines) at junction points. c_1, c_2 and $\overline{P_2P_4}$ constitute a component.

2.1.2 Implementation of SAT

The SAT of a shape *S* can be approximated by the *constrained Delaunay Triangulation* (CDT) [17, 18] over *Sí*. *Sí* here is the polygonization of the shape S. In the approximation, the maximal disks are replaced by circumcircles of Delaunay triangles (D-triangles). The triangles contained in *Sí* are called *internal triangles* (*I-triangle*s), and the rest are called *external triangles* (*E-triangle*s). The D-triangles can be classified into three kinds of triangles in terms of the number of external edges in a triangle. A D-triangle with two external edges is called a *terminal triangle* (*T-triangle*). A D-triangle with one external edge is called a *sleeve triangle* (*S-triangle*). Finally, a D-triangle that has no external edges is called a *junction triangle* (*J-triangle*) [14]. We refer here to an *external edge* as an edge of an E-triangle not shared by other E-triangles or an edge of an I-triangle not shared by other I-triangles

and an *internal edge* is an edge shared by two E-triangles or two I-triangles. The discrete symmetric axis (skeleton) consists of a collection of the centers of the circumcircles of D-triangles. We call the centers as *Delaunay centers*. An end point, a junction point and a normal point is the Delaunay center of a T-triangle, a J-triangle and a S-triangle respectively. External edges consist of the polygonal boundary in a primary skeleton before pruning. Figure 2 illustrates an example of classified Delaulay triangles, edges and the skeleton.

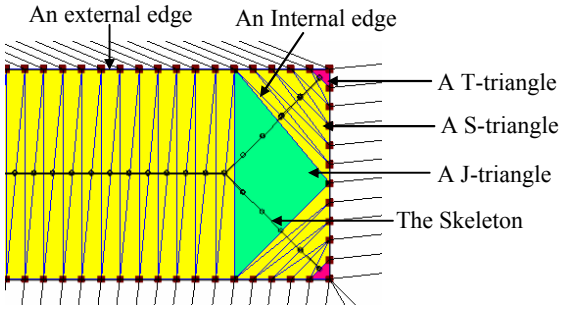

Figure 2 The illustration of internal triangles (filled triangles), external triangles (unfilled triangles), a terminal triangle (T-triangle), a sleeve triangle (S-triangle) and a junction triangle (J-triangle), an internal edge and an external edge. The skeleton is also shown.

The components of a shape in a discrete SAT consist of limbs and torsos. A *limb* is a chain complex of edge shared triangles, of the form **T S . . S J** or **J S . . S T** and a *torso* is a chain complex of edge shared triangles, of the form **J S. . S J**, where **J**, **T**, and **S** stand for a J-triangle, a T-triangle and a S-triangle, respectively (See Figure 3 for a limb and a torso in a rectangle).

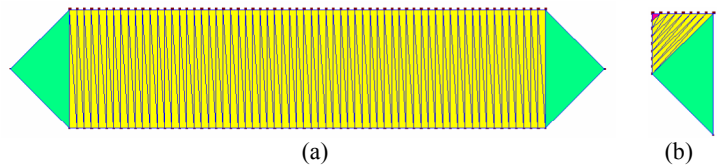

(a) (b)

Figure 3 (a) A torso; (b) A limb.

A component is expressed mathematically as : $B = \{t^0, t^1, ..t^{n-1}\}$, where $t^j = \{v_1^j, v_2^j, v_3^j\}$ is the $(j+1)$th triangle in a chain of edge-shared triangles with vertices v_1^j, v_2^j, v_3^j , $j = 0, 1, 2, .., n-1$. $v_k^j = \{x_k^j, y_k^j\}$, $k = 1, 2, 3$ with x_k^j, y_k^j being rectangle coordinate of v_k^j. t^{n-1} is a J-triangle. B is a limb when t^0 is a T-triangle or a torso when t^0 is a J-triangle. n is the number of triangles in B .

B is measured by its width $w(B)$, position $y(B)$, collinearness $\Delta y(B)$ and orientation $\alpha(B)$. They are defined as follows:

$$w(B) = \max_{0<j<n-1} \{\max_{k=1,2} \{|v_1^j - v_k^j| \mid v_1^j, v_k^j \in t^j\}\} \quad (1)$$

$$y(B) = \min_{0 \le j < n} \{y^j\} \quad (2)$$

$$\Delta y(B) = \max_{0 \le j < n} \{y^j\} - y(B) \quad (3)$$

$$\alpha(B) = o(cen(t^0) - cen(t^{n-1})) \,|\, t^0, t^{n-1} \in B \qquad (4)$$

where, $w(B)$ is the maximum edge-length of triangles in B. y^j is the y coordinate of $cen(t^j)$, $cen(t^j)$ is the center of the circumcircle of the triangle t^j, $o(cen(t^0) - cen(t^{n-1}))$ is the angle between x-axis and line segment with end points $cen(t^0)$ and $cen(t^{n-1})$.

The description of limbs and torsos are in line with SAT segmentation. From a limb or torso, the simplified segments and its two sided boundaries can be extracted in terms of the Delaunay center and the external edges of S-triangles.

2.2 The Delaunay triangulation of a face shape

2.2.1 Components in a Face image

A face can be expressed as $F = \bigcup_{i=1}^{N} B_i$, where F contains a number of limbs and torsos. Some limbs are introduced by the boundary vatiations. They do not contribute significantly to the characterization of the overall face shape but create a number of artifacts in its initial SAT, which increases the complex for face shape analysis.

A limb that satisfies

$$P_B = B : n < N_B, w(B) < w_{Bth} \qquad (5)$$

where n is the number of triangles in P_B, is caused by an artifact of the blobsí contours. This type of limbs are pruned from *F*.

Usually eyebrows (some Asian faces are exceptions) or wrinkles around eyes are closer to eyes than other facial features. They are clustered into eye regions in order to simplify the inner facial feature identification. For this purpose, torsos around eyes are removed. They are horizontal-oriented torsos having narrow width. Each of them satisfies:

$$P_T = B : w(B) < w_{Tth}, |\alpha(B)| < \alpha_{th}, \Delta y(B) < \Delta h_{th}, n > N_T \qquad (6)$$

Here n is the number of triangles in P_T.

A refined (pruned) facial shape is obtained after pruning by following operation:

$$F' = (F - \{P_{Bj}\} - \{P_{Tk}\}) \cup \{t_i^{n_i - 1}\}) \quad j = 1,2,...J \;\; k = 1,2,...K \qquad (7)$$

Where J is the number of limbs that satisfy equation (5), K is the number of torsos that satisfy equation (6), $\{t_i^{n_i-1}\}$ are the J-triangles in the pruned components that will remain and evolve in the S-triangles in the refined shape. An example of face shape refinement is shown in Figure 4.

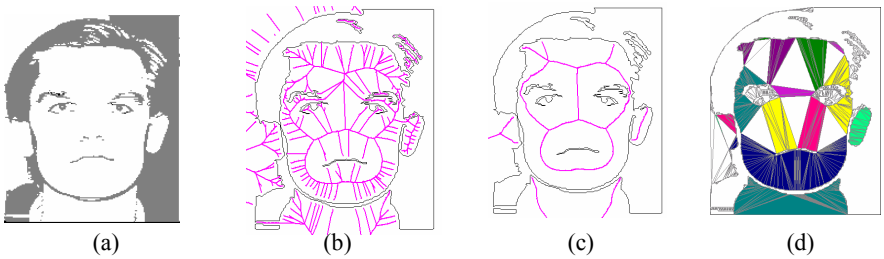

(a) (b) (c) (d)

Figure 4 Face (skin) skeleton and face shape refinement (a) A binarized face image; (b) Initial skeleton; (c) Skeleton after artifacts removing; (d) components in the face after artifacts removing. The S-triangles in each component have the same color.

2.2.2 Inner facial feature identification

New external edges and boundaries are formed after pruning, which captures the left/right eye/eyebrow regions (represented by their boundaries C_L and C_R), the mouth region (represented by its boundary C_M) and in some cases the nostril region (represented by its boundary C_N) in the face (see Figure 5(a)). The artifacts along the face boundaries are also eliminated. The new boundaries consist of c_1s and c_2s of a number of components in F'.

A specific torso will be generated for faces with different topological structures. The torso has a robust trunk and its c_1 is on one eye/eyebrow region and c_2 on another eye/eyebrow region. We call this trunk the eye-axis (see Figure 5(b)). It is roughly straight and the two-eye/eyebrow regions (C_L and C_R) containing the c_1 and c_2 of the eye-axis are symmetric to the axis.

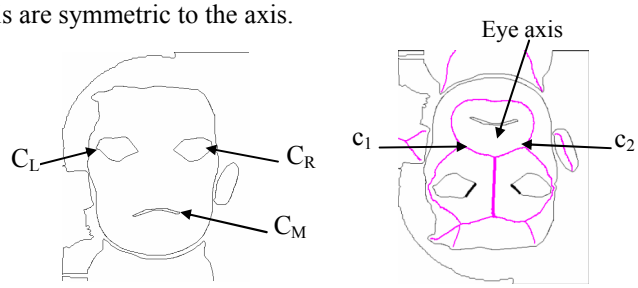

Figure 5 New region boundaries and the eye axis.

Eye axis, C_L and C_R are located through straightness and vertical measurement of a trunk and the shape and geometrical distance test of the trunk associated regions. C_M and C_N are located by calculating the relative geometric distance from C_L and C_R to the other regions.

2.3 Face boundary extraction

Face boundary (C_F) is extracted from each of the torsos that have one-sided curve (c_1) on a facial feature region. Another sided curve (c_2) contributes to the face boundary. Hair boundary on the forehead are also included in C_F. The hair boundary lies in the two sided curves c_1 and c_2 of each of the limbs above the eye regions (C_L

and C_R). We name the above torsos or limbs associated with face boundary or hair boundary the *boundary components* (See the filled trinagles in Figure 6).

Face boundary is broken at the mergence of the face skin and the background areas. A J-triangle lying in the face skin will be generated which links to a background area (See Figure 5 for an example). The edge of the J-triangle with two outer points as its end points split the face skin and the background area. This edge is regarded as the linkage of the broken face boundary.

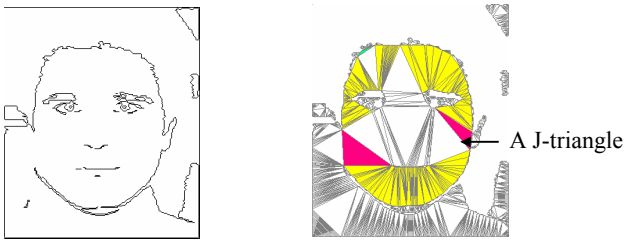

Figure 6 An edge of the J-triangle Splits the mergence of face skin and background

The trace of C_F is within the chain of E-triangles in the boundary components that have the connected external edges along the face or hair border. We denote the set of these E-triangles as U. Then,

$U = F' - I$, $I = \{t \mid t \in F' \text{ and } v_1, v_2, v_3 \in C_I\}$, where I is the set of all the triangles in Fi with each triangleís three vertices on the boundaries of inner facial feature regions.

3 Experimental results

Test images are chosen from Yale Face Database B [18]. Yale Face Database B contains single light source images of 10 subjects each seen under frontal pose and the angle between the light source direction and the camera axis is under 10^0, which yields clear face edges and inner facial features.

The Delaunay Triangulation is established on the binarization of a grayscale face image, which consists of a number of blobs. The inner facial features and face border are among the blobs.

Figure 7 showes extracted face boundaries for several tested images. The shapes of chins vary individually. Some of them are thin or sharp, some of them are broad or flat. In Figures 7 (e, f, g) the extracted boundary is broken near the ears or the neck. The missing edges in Figures 7 (e, f) are not too long, and in this case the gap can be filled by directly connecting the nearby boundary segments. In Figure 7 (j) the gap is too large, and the direct link will obviously deviate the face boundary, causing distortion at the broken position. The forehead is hidden by its long front hairs in Figure 7 (c), the end of the hairs is traced instead of the forehead. Also in Figure 7 (d), the hairs affect the edge of the forehead, and some boundary details of hairs are included. In Figure 7 (j), the edge of mustache near the chin is strong, the mustache curve near the chin replaces chin curve.

The chins have similar intensity with the background for some of the images in Figures 7 (i, j). As a result, the traced boundary cuts the chin curves or highly deviates the chin.

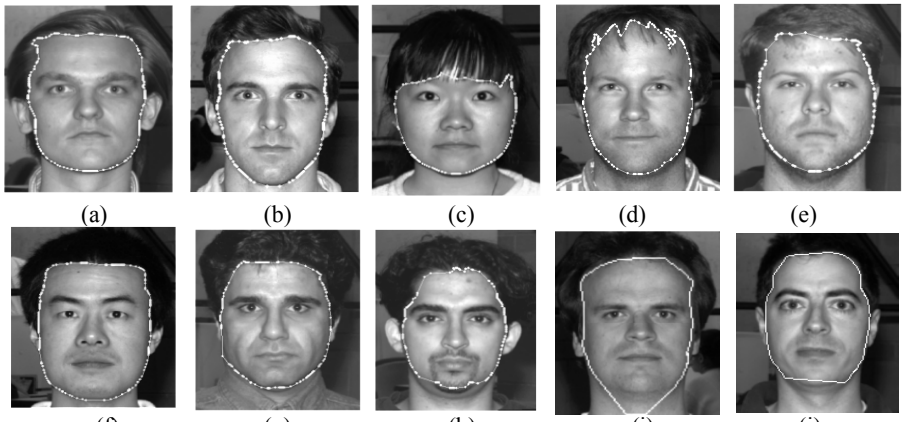

Figure 7 Extracted Face boundaries for images in Yale B database.

The tested processing time for the images of Figure 7 is tabulated in Table 1 A Pentium III processor is used at a clock frequency of 800MHz.

Table 1 Processing time of images in Figure 7.

Test image	*(a)*	*(b)*	*(c)*	*(d)*	*(e)*	*(f)*	*(g)*	*(h)*	*(i)*	*(j)*
Binarization (s)	*1.28*	*1.28*	*1.28*	*1.28*	*1.28*	*1.28*	*1.30*	*1.28*	*1.28*	*1.28*
Feature location (s)	*0.61*	*0.62*	*0.87*	*0.61*	*0.98*	*0.69*	*0.78*	*0.62*	*0.49*	*0.73*
Boundary trace(s)	*0.20*	*0.17*	*0.34*	*0.34*	*0.25*	*0.26*	*0.23*	*0.26*	*0.21*	*0.23*
Total time(s)	*2.09*	*2.07*	*2.49*	*2.23*	*2.51*	*2.23*	*2.31*	*2.16*	*1.98*	*2.24*

The most time consuming of the processes is the binarization.

A comparison is made between the proposed method and that reported in [10] using face images obtained from Bern database [19]. Table 2 gives the applicability and limitation between the two methods.

Table 2 Comparison of the applicability and limitation between the two methods

Method	Reference	Limitation
Hu et al	Front-up, plain background, glasses	Rotation, tilt
Proposed method	Complex background, Front-up	Glasses, rotation

Clear face border is crucial for extracting fine face boundary in both methods. In Figure 8, the face has distinct face edge, smoothed and well-fitted results (Figures 8 (a_1) and (a_2)) are obtained from both methods.

In the proposed method, only the Delaunay edges related to the Delaunay triangles that link inner facial features and the face boundary are recorded. Therefore, the deviation of traced boundary from face border is avoided and the traced boundary is closed. In Hu et alís method, however, it is difficult to determine the two ending points of the segment of the bottom boundary. And chin boundaries do not match all the faces, especially for rotated faces (See Figure 8(b_2)). Zigzag curves may be generated when face edges are weak or noise (such as hairs) exists. An example is shown in Figure 8 (c_2).

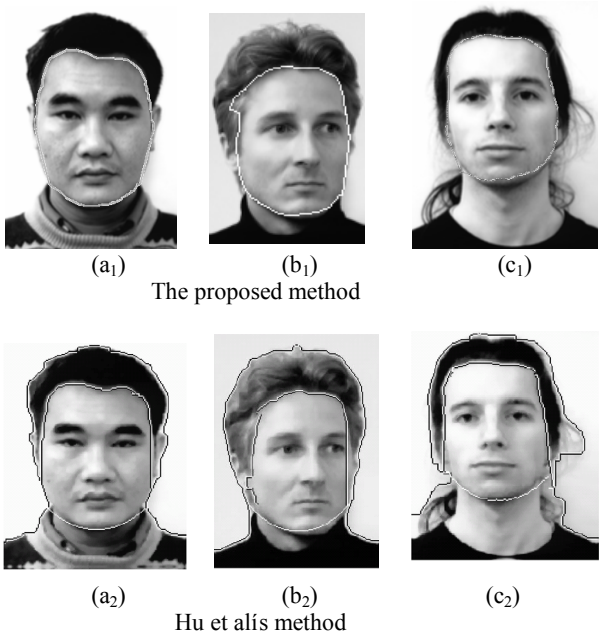

(a_1) (b_1) (c_1)

The proposed method

(a_2) (b_2) (c_2)

Hu et alís method

Figure 8 Comparison of the proposed method with Hu et al ís method [10].

The problem to be explored by the proposed method is the limitation of the existing of glasses.

4 Conclusion

In this paper, we have developed a novel technique to make use of a chain of internal-edge-shared Delaunay triangles that can be used to quantitatively and topologically measure a shape, especially suitable for the analysis of a symmetric shape like a human face. The facial features associated with the specific component can be identified by the symmetry related distance analysis and then the face boundaries are traced by the components formed by face boundaries and inner facial features. The method is suitable for arbitrary face shapes and tolerant face boundaries broken caused by the weak edges in a face image.

References

1. M. H. Yang, D. J. Kriegmen and N. Ahuja, Detecting faces in images: a survey, *IEEE transactions on pattern analysis and machine intelligence*, Vol 24, no. 1, pp 34-58, 2002.
2. Andreas Lanitis, Chris J. Taylor, and Timothy F. Cootes, Automatic Interpretation and Coding of Face Images Using Flexible Models, *IEEE transactions on pattern analysis and machine intelligence*, Vol. 19, no. 7, pp 743-756, 1997.
3. S. Boursas and H. Yan, Chin extraction in colour frontal-view face images, *Digital Image Computing Techniques and Applications*, 21-22, Melbourne, Australia, pp 1-6, 2002.
4. G. Davis, H. Ellis and J. Sheferd, Perceiving and remembering faces, *Press Series in cognition and perception. Academic press*, London, 1981.
5. T. Sakai, M. Nagao and T. Kanade, Computer analysis and classificaion of photographs of human faces, *Proc. First USA-Japan computer conf.*, pp 245-256, 1986.
6. M. Kass, A. Witkin, D. Terzopoulos, Snake: active contour models, Int. J. Comput. Vision 1 (4) pp 321 – 331, 1988.
7. K. Sobotta and I.Pitas. Segmentation and tracking of faces in color images. In *Proc. 2nd Int. Conf. On auto Face and Gesture Recogn.,* Vermont, IEEE Comp. Soc. Press pp 236-241, 1996.
8. K. M. Lam and H. Yan, Fast algorithm for locating head boundaries, *J. Electrical Imaging* 3 (4), pp 351-359,1994.
9. T. Akimoto, Y. Suenaga, and R. S.Wallace, ì Automatic creation of 3-D facial models,î *IEEE Comput. Graph. Applicat.*, vol. 13, no. 5, pp. 16ñ22, 1993.
10. J. Hu, H. Yan and M. Sakalli, Locating head and face boundaries for head-shoulder images, *Patter Recognition*, 32, pp 1317-1333, 1999.
11. H. Blum, ì A transformation for extracting new descriptors of shape,î *Proc. Symp. Models for the Perception of Speech and Visual Form* (W.W. Dunn, ed.), MIT Press, Cambridge, MA, pp. 362ñ380, 1967.
12. Blum, H. and R. N. Nagel shape description using weighted symmetric axis features, *Pattern Recognition*, 10, pp 167-180, 1978.
13. J. W. Brandt and V. R. Algazi, Continuous skeleton computation by Voronoi diagram, *Computer Vision, Graphics, and Image Processing*, Vol 55, no 3, pp 329-338, 1992.
14. L. Prasad, morphological analysis of shapes, http://cnls.lanl.gov/Highlights/1997-07/html/July_97.html
15. R. L. Ogniewicz, Discrete Voronoi Skeletons, Hartung-gorre Verlag, Konstanz, Germany, 1993
16. B. Kimia, Symmetry-Based Shape Representations, http://www.lems.brown.edu/vision/Presentations/Kimia/IBM-Oct-99/talk.html
17. L. P. Chew, Constrained Delaunay Triangulation, *Algorithmica*, Vol 4, pp 97-108, 1989.
18. A. Okabe, B. Boots and K. Sugihara, Spatial Tessellations-Concepts and Applications of Voronoi Diagrams, Second Edition, *Wiley Series in probability and statistics*, 2000
19. http://cvc.yale.edu/projects/yalefacesB/yalefacesB.html
20. ftp://iamftp.unibe.ch/pub/Images/FaceImages/